Accepted Manuscript

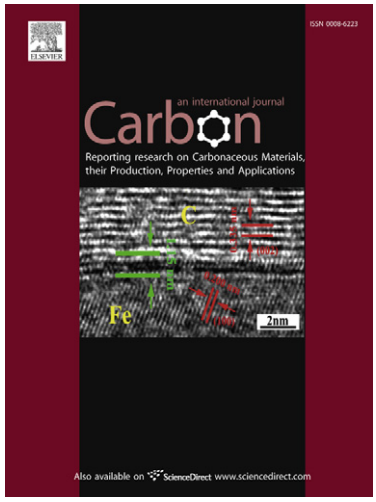

Mechanical Properties of Individual Electrospun Polymer-Nanotube Composite NanoFibers

Dorothee Almecija, David Blond, John E Sader, Jonathan N Coleman, John J Boland

PII: S0008-6223(09)00242-5
DOI: 10.1016/j.carbon.2009.04.022
Reference: CARBON 5297

To appear in: *Carbon*

Received Date: 7 January 2009
Revised Date: 26 March 2009
Accepted Date: 13 April 2009

Please cite this article as: Almecija, D., Blond, D., Sader, J.E., Coleman, J.N., Boland, J.J., Mechanical Properties of Individual Electrospun Polymer-Nanotube Composite NanoFibers, *Carbon* (2009), doi: 10.1016/j.carbon.2009.04.022

Mechanical Properties of Individual Electrospun Polymer-Nanotube Composite NanoFibers

Dorothee Almecija[1,2], David Blond[2,3], John E Sader[4], Jonathan N Coleman[2,3*] and John J Boland[1,2*]

[1]*School of Chemistry, Trinity College Dublin, Dublin 2, Ireland,*

[2]*Centre for Research on Adaptive Nanostructures and Nanodevices, Dublin 2, Ireland,*

[3]*School of Physics, Trinity College Dublin, Dublin 2, Ireland,*

[4]*Department of Mathematics and Statistics, University of Melbourne, Parkville, Victoria 3010, Australia*

Abstract

Singlewalled carbon nanotube / polyvinylalcohol composite nanofibers were electro-spun onto a silicon surface pre-patterned with trenches. These nanofibers were prepared with different loadings of SWCNTs and had radii between 20 and 40nm. Individual fiber sections were pinned across the trenches and laterally loaded by an AFM tip to yield mechanical response curves. A simple model was exploited to extract the tensile mechanical properties from the lateral force-displacement data. Depending on the fibre composition, the tensile modulus was found to be between 3 and 85 GPa. In addition we have prepared fibers with tensile strength of up to 2.6 GPa. Such optimised fibers break at strains of ~4% and exhibit toughness of up to 27 MJ/m^3.

1. Introduction

Electrospinning has been used since 1934(1) to continuously produce low diameter polymer fibers from polymer solutions or melts(2). However, in recent years this technique has become more popular, principally to produce low density, porous membranes. By continuous electrospinning of fibers onto a

* Corresponding Authors: E-mail address: colemaj@tcd.ie (J.N. Coleman). Tel.: +353 18963859; fax: +353 16711759.
E-mail address: jboland@tcd.ie (J. J. Boland). Tel.:+353 1896 3140; fax: +353 18963142

stationary electrode, it is possible to build up a network which can eventually develop into a membrane some hundreds of microns thick. Potential applications suggested for these membranes range from use as bone(3) or tissue-engineering scaffolds(4) to battlefield dressings(5) and protective clothing(6). For many of these applications, mechanical strength and toughness are extremely important as even partial failure could have catastrophic consequences. While the topological properties of the network have a significant influence on its mechanical properties(7), the strength of the membrane is ultimately limited by the strength of the individual fibers. As such, significant work has gone into reinforcing the individual fibers through the incorporation of carbon nanotubes(7-15).

Well dispersed, well aligned nanotubes, which have been chemically modified to maximise polymer-nanotube stress transfer(16) are expected to be the ideal filler for mechanically reinforced composites(17). Due to their enforced alignment, nanotubes have shown significant promise as fillers in fibers(18-21). Polymer-nanotube composite fibers with strengths of up to 4.2GPa have been demonstrated(21). Thus we expect that individual nanotube-reinforced, electrospun fibers can attain high strengths and stiffnesses. However, electrospun fibers typically have sub-micron diameters, making it very difficult to measure their tensile properties. A small number of studies have appeared and strengths as high as 80MPa have been reported for electrospun PMMA-nanotube fibers(22). However, we feel that it should be possible to produce even stronger fibers by using alternative matrices. In recent years, a number of papers have appeared demonstrating the strength of polyvinylalcohol (PVA)-nanotube fibers(18, 20) and films(23, 24). In addition, surprisingly strong electrospun membranes have been produced from PVA(7).

In this work we electrospin very sparse networks of PVA-nanotube nanofibers onto silicon substrates with pre-prepared micron sized trenches. We use an atomic force microscope to exert a lateral force on individual fibers while monitoring both force and displacement. Using a simple tensile model, we generate the tensile properties of the fibers from this force displacement data. For optimised nanotube loading levels we have observed fibers with strengths and moduli of up to 2.6 GPa and 85 GPa respectively.

2. Experimental

The PVA used in this work was purchased from Sigma Aldrich (M_w=30 000-70 000 $gmol^{-1}$). Water-soluble PABS-SWCNTs (www.carbonsolution.com) were chosen to achieve high-quality nanotube dispersions in the PVA/water solutions(7, 16). A concentration of 250gL^{-1} of PVA was used to prepare PVA/PABS-SWCNTs solutions with various mass fractions of SWCNTs (from 1 wt% down to 0.06wt%). Typically, each mass fraction of CNTs was first dispersed in 20mL of distilled water using a high–power sonic tip for 5 min (VibraCellCVX, 750W, 20%, 20kHz). Subsequently, each dispersion was placed in a lower-power sonic bath for 3h (Branson 1510, 42 kHz, 80W). Next, PVA powder was added slowly to the solution and crushed with a spatula in order to minimise PVA agglomeration. Again, the solution was placed under the sonic tip for 5min to break up any remaining polymer aggregates before placing it in a sonic bath for further 24h until complete dissolution occurred. Finally, the solutions were sonicated with a sonic tip for 2min immediately prior to electrospinning.

The electrospinning set up consisted of a 20mL glass syringe with a 16 gauge stainless steel needle that was positioned on a horizontally moveable structure. A stationary stainless steel plate (15cm × 15cm) was used as a collector. For mechanical measurements, it was necessary to deposit fibers onto pre-patterned silicon wafers with arrays of 5µm wide trenches. Thus, these silicon substrates were placed just in front of the steel collector. For all the experiments carried out with this setup, the distance between the needle and the collector was set at 20cm. The high voltage was provided by a Brandenburg high voltage generator. For each run, the voltage was kept at 20 kV. The needle was positively charged while the collector was grounded. A syringe pump (KDS 200 syringe pump) was used to ensure a constant flow rate at 0.003$mLmin^{-1}$.

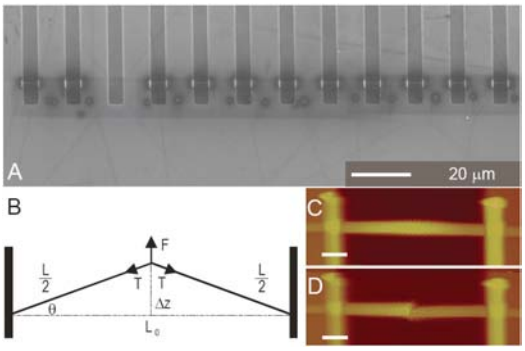

Figure 1. A) SEM image of a single polymer-nanotube composite fiber spanning several trenches on a SiO_2 substrate. B) Schematic showing the mechanical measurement technique and the parameters involved in the calculation of the tensile model. C) AFM image of a fiber spanning over a trench before and D) after fracture. The scale bar is 1µm.

Solutions were electrospun for a very short time (~45 s), resulting in a low density mesh of fibers with radii between 20 and 40 nm. Mechanical measurements were performed following a technique previously developed for metallic and semiconducting wires(25-27). Scanning electron microscopy was used to monitor both the density and the position/alignment of the nanofibers across the trenches. Fibers spanning the trenches perpendicularly were pinned down by electron beam induced deposition of platinum inside a scanning electron microscope chamber(25) as shown on Figure 1A. Both the diameter and suspended length were measured for all fibers using an atomic force microscope (AFM). Fibers, pinned on either side of a trench, were laterally loaded by an AFM tip while the force-displacement (F-Δx) curves were recorded. Rectangular cantilevers with resonance frequencies of around 300 kHz and lateral and normal force constants of 100-300 Nm^{-1} and 20-40 Nm^{-1} respectively were used. For the relative directions of force, displacement and fiber, see Figure 1B. An x-y-z closed loop scanner was used to position the tip extremely accurately at the loading point (centre of spanning fibre) and deep enough into the trench to avoid slippage. For each mass fraction 15 to 20 fibers were tested. Figures 1C and 1D are AFM micrographs of a fiber, before and after mechanical loading.

3. Results and Discussion

3.1 Force-displacement measurements

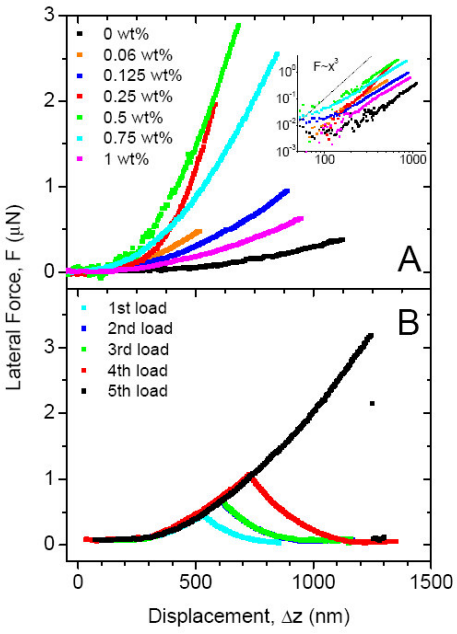

Figure 2A shows representative F-Δx curves for fibers of different CNT mass fraction during lateral loading. This behaviour is characteristic of double-clamped beam configurations for an elastic wire. All fibers fracture at large displacement (on average 30 times their radii) without plastic deformation and always break at the centre, as shown in the AFM micrographs in Figure 1C and D. Figure 2B shows the F-Δx curves for a 1wt% fiber loaded 5 times until fracture. The reversible behaviour demonstrates the absence

Figure 2. Lateral force versus displacement curves for some of the fibers studied. A) Representative lateral force versus displacement curves for fibers filled with different nanotube mass fractions. Inset: the same graph displayed on a log-log scale. B) Lateral force versus displacement curves for a single fiber, strained repeatedly to different maximum values of Δx.

of plasticity at displacements of <700nm (<4% tensile strain). In addition, this reversible behaviour coupled with the fact that fibers always break at the point of loading (i.e. center of suspended fiber) implies the absence of pull-out at the Pt clamps points. However, we note that pull-out has previously been used to measure interfacial shear strength(28). The simplest data which can be obtained from these curves are the force and displacement at break. These parameters are shown in Figure 3A and B respectively, as a function of nanotube content. For low mass fractions, the force to break is increased on adding CNTs, while the displacement at break is reduced. Some saturation is observed at higher mass fractions, possibly due to nanotube aggregation.

3.2 Theoretical Considerations

A theoretical model needs to be developed to extract the tensile mechanical properties of these fibers from the F-Δx data. The simplest possible model considers the fiber as an elastic string(29) and gives a relationship between the applied load, F, and the perpendicular displacement, Δz, as well as expressions for the tensile strength, σ_B, and the strain at break, ε_B. In addition, by assuming the material to fail by brittle fracture, we can obtain lower bounds for both tensile elastic modulus, E, and toughness T_E. In what follows, the subscript B denotes the value of a quantity when the fiber breaks. We assume that the AFM tip applies the lateral force, F, to the centre of the fiber, in a direction perpendicular to the initial fiber length as shown in Figure 1B. The elastic string analysis gives a relationship between the lateral force and the perpendicular displacement, Δz:

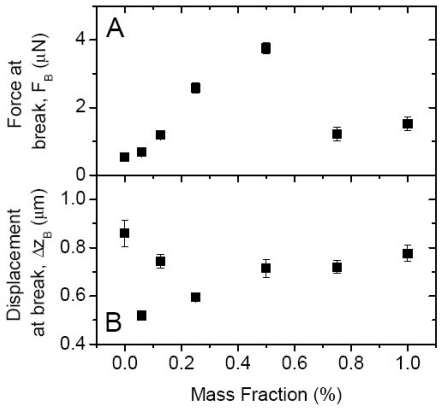

Figure 3. Mean values for A) Force at break and B) displacement at break, as a function of nanotube mass fraction for all the fibers studied in this work. In both cases the error bars represent the standard errors calculated from 10-15 measurements.

$$F \approx 8\pi E R^2 \Delta z^3 / L_0^3 \qquad \text{Eq 1}$$

where E is the tensile modulus of the fiber, R is the fiber radius and L_0 is the initial fiber length. Assuming the tension in the fiber can be written as $T = F / 2Sin\theta$ and writing the fiber tensile strength as $\sigma_B = T_B / \pi R^2$, (T_B is the tension when the fiber breaks) we can express the tensile strength as

$$\sigma_B \approx F_B L_0 / 4\pi R^2 \Delta z_B \qquad \text{Eq 2}$$

where F_B and Δz_B are the values of lateral force and perpendicular displacement when the fiber breaks. Similarly, we can write the strain at break as

$$\varepsilon_B = (L_B - L_0) / L_0 \approx 2\Delta z_B^2 / L_0^2 \qquad \text{Eq 3}$$

(L_B is the fiber length on fracture). The force displacement curves show sub-cubic behaviour (quite close to quadratic), as seen on the inset in Figure 2A, which we believe is due to a slightly sub-linear relationship between tensile stress and strain. We attribute this to non-Hookian behaviour, often observed for polymers, rather than plasticity. Repeated stretching of the fibers show no signs of plasticity for Δz<700nm (ε<4%) at least. However, without precise knowledge of the constitutive equation for this material, modelling of such non-ideal behaviour is extremely difficult. In the absence of further knowledge, this tensile model is a valid approximation which directly gives values for σ_B and ε_B as described above. However we note that the non-cubic behaviour observed in the measured data makes it inappropriate to use equation 1 to find E. To estimate E we must make the approximation that $\sigma \propto \varepsilon$ over the whole strain range. This gives us an under estimate of the Young's modulus from $E \approx \sigma_B / \varepsilon_B$. Similarly, we can get an under estimate of the toughness from $T_E \approx \sigma_B^2 / 2E$.

3.3 Data Analysis

The tensile modulus was calculated for each fiber using the tensile model as described above. The moduli values for individual nano-fibers varied between 3 and 85 GPa, depending on the SWCNT mass fraction with significant spread in the moduli for different fibers of the same mass fraction. Over the range of mass fractions studied, the mean moduli varied between 10 and 50 GPa. This range is not unexpected

since PVA/SWNT coagulation spun fibers have shown similar moduli, varying between 10 and 80 GPa(18-20).

The strengths of the individual composite fibers were calculated for all mass fractions using the tensile model described in Eq. (2). The individual fiber strength varied between 0.26 and 2.6 GPa. However, the mean strength calculated for each mass fraction varied from 0.5 GPa to 1.4 GPa. In addition, the mechanical properties of these nanofibers are maximised for SWCNT mass fractions of 0.06% and 0.125%.

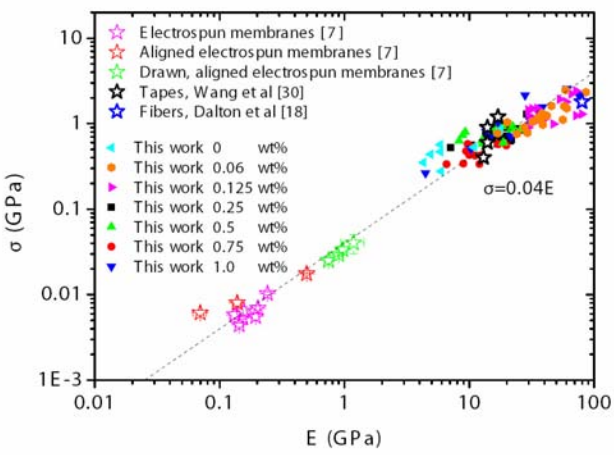

Figure 4. Plot of fiber tensile strength versus fiber tensile modulus. Also shown are data, taken from the literature, for PVA/nanotube composites in form of fiber-like material or aligned tapes (stars). Note that the literature data tend to sit on a straight line defined by σ=0.04E.

We note that the model used to calculate the tensile strength is approximate as described above. In addition, to calculate the modulus we resort to assuming purely brittle failure, a significant simplification. We can test the validity of these assumptions fairly simply by noting that, for a range of reported PVA-nanotube composites(7, 18, 30), the strength scales linearly with the modulus ($\sigma_B=0.04E$) as shown in Figure 4. For comparison, we plot the calculated strength versus the calculated modulus for our fibers in Figure 4. Here, the strength scales approximately linearly with the modulus as expected. However, more importantly the fiber data lies close to the straight line described by $\sigma_B=0.04E$ which is typical for PVA- nanotube composites. This agreement between our results and those available in the literature give us confidence that our model works reasonably well.

Mean tensile modulus, tensile strength, toughness and strain at break for these fibers as a function of nanotube volume fraction are presented in Figure 5. Note that we have transformed the nanotube content from mass fraction to volume faction to facilitate analysis using the rule of mixtures. Also we remember that, within the framework of the model used, both modulus and toughness are underestimates. For both modulus and strength (Figure 5A and B), significant increases are observed at low SWCNT content

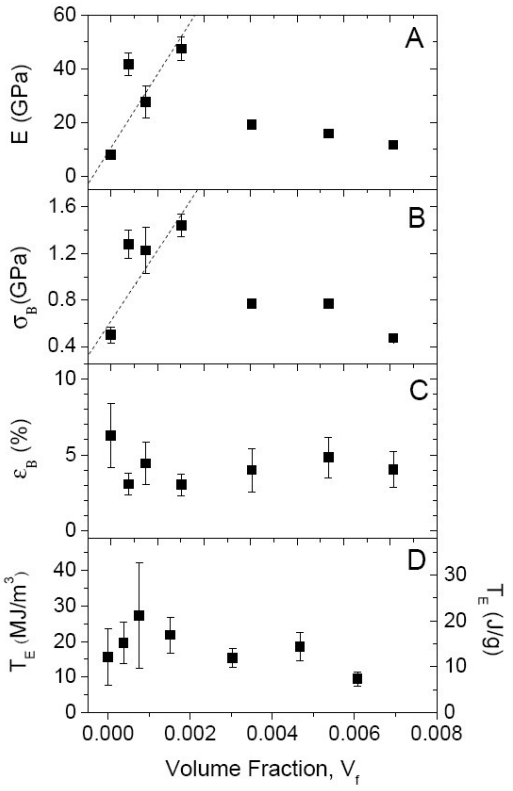

Figure 5. Data calculated using the tensile model, plotted as a function of composite mass fraction: A) Young's modulus E, B) tensile strength σ_B, C) strain at break ε_B and D) toughness T_E. The right axis shows the toughness plotted by mass (calculated taking ρ_{PVA}=1300 kg/m^3). The error bars are the standard errors calculated from 10-15 measurements.

(<0.2vol%), with mean modulus and strength reaching values as high as 50 GPa and 1.4 GPa respectively. These values are at the high end of what has been observed for polymer-nanotube composite fibers(23). The rate of increase of both modulus and strength in this regime are dE/dV_f~27 TPa and $d\sigma_B/dV_f$~600 GPa respectively. These extremely high values cannot be explained by the standard Rule of Mixtures which can account for values of dE/dV_f and $d\sigma_B/dV_f$ no larger than the nanotube modulus and strength respectively (~1TPa and ~100GPa)(17). It is likely that some other form of reinforcement is present to explain these results. A likely possibility is nanotube-nucleated polymer ordering which is often observed in PVA based composites(31) and is known to result in significantly enhanced mechanical properties(17, 24). At volume fractions above 0.2vol%, both modulus and strength tend to fall off slightly. This is generally attributed to nanotube aggregation, which is unsurprising given that adjacent aligned nanotubes are typically only ~20 nm apart at a volume fraction of 0.2vol%.

The data for fiber strain at break and toughness are shown in Figure 5C and D. The strain at break, ε_B, was 6% for a PVA only fiber and falls off slightly as nanotubes are added, saturating at ~4%. The PVA-only fibers displayed toughnesses of ~15 MJ/m^3. On adding nanotubes, the toughness increased slightly to a maximum of 27 MJ/m^3, equivalent to 20 J/g. At higher mass fractions, the toughness fell off, in line with the fall off in strength. It should be noted that these fibers display reasonably high toughness. For comparison, Kevlar fibers have toughness in the region of 35 J/g(32). Although our fibers are not super-tough, as has been reported for SWCNT-PVA fibers produced by coagulation spinning(18), they have one significant

advantage. Their toughness comes from energy absorbed at low strain (<4%) as is the case for Kevlar and other tough fibers(33). By contrast, super-tough fibers tend to be tough because they are ductile(18). However, in many cases they absorb very little energy at strains below 5%, making them unsuitable for many applications. Thus, these electrospun fibers may be useful for ballistic-type applications requiring the absorption of large quantities of energy over small distances.

4. Conclusions

We have developed a method to deposit electrospun nano-fibers across pre-prepared trenches on silicon substrates. Using an AFM to apply a lateral force to the centre of the fiber we measure both force and displacement as the fiber is strained. We present a simple model which we use to generate the tensile properties; modulus, strength, strain at break and toughness from the force displacement data. We find the tensile properties are optimised around 0.05vol% nanotubes. We have observed maximal strengths and moduli of 2.6 GPa and 85 GPa respectively. Optimised fibers break at strains of ~4% having absorbed ~27 MJ/m^3.

Acknowledgments

We would like to acknowledge both IRCSET and Science Foundation Ireland for continuing financial support under contracts 06/IN.1/I106 and 07/IN.1/I1772, and funding by the Australian Research Council Grants Scheme.

.

References

1. Formhals A, inventor f lorty, assignee. Artificial thread and method of producing same. USA patent 2187306. 1937.

2. Ramakrishna S, Fujihara K, Teo W-E, Lim T-C, Ma Z. An Introduction to Electrospinning and Nanofibers. Singapore: World Scientific Publishing Co Pte Ltd; 2005.

3. Meechaisue C, Wutticharoenmongkol P, Waraput R, Huangjing T, Ketbumrung N, Pavasant P, et al. Preparation of electrospun silk fibroin fiber mats as bone scaffolds: a preliminary study. Biomed Mater. 2007;2(3):181-8.

4. Christopher TG, Daniel JJ, Christopher A, Chris A, Trevor R. Method to determine the spring constant of atomic force microscope cantilevers. Review of Scientific Instruments. 2004;75(2):565-7.

5. Ignatova M, Manolova N, Rashkov I. Novel antibacterial fibers of quaternized chitosan and poly(vinyl pyrrolidone) prepared by electrospinning. Eur Polym J. 2007 Apr;43(4):1112-22.

6. Sundarrajan S, Ramakrishna S. Fabrication of nanocomposite membranes from nanofibers and nanoparticles for protection against chemical warfare stimulants. J Mater Sci. 2007 Oct;42(20):8400-7.

7. Blond D, Walshe W, Young K, Blighe FM, Khan U, Almecija D, et al. Strong, tough, electrospun polymer-nanotube composite membranes with extremely low density. Adv Funct Mater. 2008 Sep;18(17):2618-24.

8. Dror Y, Salalha W, Khalfin RL, Cohen Y, Yarin AL, Zussman E. Carbon nanotubes embedded in oriented polymer nanofibers by electrospinning. Langmuir. 2003 Aug;19(17):7012-20.

9. Hanrath T, Korgel BA. Chemical surface passivation of Ge nanowires. J Am Chem Soc. 2004 Dec;126(47):15466-72.

10. Zhou W, Wu Y, Wei F, Luo G, Qian W. Elastic deformation of multiwalled carbon nanotubes in electrospun MWCNTs-PEO and MWCNTs-PVA nanofibers. Polymer. 2005;46(26):12689-95.

11. Jeong JS, Moon JS, Jeon SY, Park JH, Alegaonkar PS, Yoo JB. Mechanical properties of electrospun PVA/MWNTs composite nanofibers. Thin Solid Films. 2007;515(12):5136-41.

12. F. Ko, Gogotsi Y, Ali A, Naguib N, Ye H, Yang GL, et al. Electrospinning of Continuous Carbon Nanotube-Filled Nanofiber Yarns. Advanced Materials. 2003;15(14):1161-5.

13. McCullen SD, Stevens DR, Roberts WA, Ojha SS, Clarke LI, Gorga RE. Morphological, Electrical, and Mechanical Characterization of Electrospun Nanofiber Mats Containing Multiwalled Carbon Nanotubes. Macromolecules. 2007;40(4):997-1003.

14. Minoo N, Tong L, Wendy T, Liming D, Xungai W. Effects of MWNT nanofillers on structures and properties of PVA electrospun nanofibres. Nanotechnology. 2007(22):225605.

15. Sen R, Zhao B, Perea D, Itkis ME, Hu H, Love J, et al. Preparation of Single-Walled Carbon Nanotube Reinforced Polystyrene and Polyurethane Nanofibers and Membranes by Electrospinning. Nano Lett. 2004;4(3):459-64.

16. Amiran J, Nicolosi V, Bergin SD, Khan U, Lyons PE, Coleman JN. High quality dispersions of functionalized single walled nanotubes at high concentration. J Phys Chem C. 2008 Mar;112(10):3519-24.

17. Coleman JN, Khan U, Blau WJ, Gun'ko YK. Small but strong: A review of the mechanical properties of carbon nanotube-polymer composites. Carbon. 2006 Aug;44(9):1624-52.

18. Dalton AB, Collins S, Munoz E, Razal JM, Ebron VH, Ferraris JP, et al. Super-tough carbon-nanotube fibres - These extraordinary composite fibres can be woven into electronic textiles. Nature. 2003 Jun;423(6941):703-.

19. Miaudet P, Badaire S, Maugey M, Derre A, Pichot V, Launois P, et al. Hot-drawing of single and multiwall carbon nanotube fibers for high toughness and alignment. Nano Lett. 2005 Nov;5(11):2212-5.

20. Vigolo B, Poulin P, Lucas M, Launois P, Bernier P. Improved structure and properties of single-wall carbon nanotube spun fibers. Appl Phys Lett. 2002 Aug;81(7):1210-2.

21. Kumar S, Doshi H, Srinivasarao M, Park JO, Schiraldi DA. Fibers from polypropylene/nano carbon fiber composites. Polymer. 2002 Mar;43(5):1701-3.

22. Liu LQ, Tasis D, Prato M, Wagner HD. Tensile mechanics of electrospun multiwalled nanotube/poly(methyl methacrylate) nanofibers. Advanced Materials. 2007 May;19(9):1228.

23. Coleman JN, Cadek M, Ryan KP, Fonseca A, Nagy JB, Blau WJ, et al. Reinforcement of polymers with carbon nanotubes. The role of an ordered polymer interfacial region. Experiment and modeling. Polymer. 2006 Dec;47(26):8556-61.

24. Coleman JN, Cadek M, Blake R, Nicolosi V, Ryan KP, Belton C, et al. High-performance nanotube-reinforced plastics: Understanding the mechanism of strength increase. Adv Funct Mater. 2004 Aug;14(8):791-8.

25. Wu B, Heidelberg A, Boland JJ. Mechanical properties of ultrahigh-strength gold nanowires. Nat Mater. 2005 Jul;4(7):525-9.

26. Heidelberg A, Ngo LT, Wu B, Phillips MA, Sharma S, Kamins TI, et al. A generalized description of the elastic properties of nanowires. Nano Lett. 2006 Jun;6(6):1101-6.

27. Ngo LT, Almecija D, Sader JE, Daly B, Petkov N, Holmes JD, et al. Ultimate-strength germanium nanowires. Nano Lett. 2006 Dec;6(12):2964-8.

28. Nuriel S, Katz A, Wagner HD. Measuring fiber-matrix interfacial adhesion by means of a 'drag-out' micromechanical test. Composites Part A: Applied Science and Manufacturing. 2005;36(1):33-7.

29. Walters DA, Ericson LM, Casavant MJ, Liu J, Colbert DT, Smith KA, et al. Elastic strain of freely suspended single-wall carbon nanotube ropes. Appl Phys Lett. 1999;74(25):3803-5.

30. Wang Z, Ciselli P, Peijs T. The extraordinary reinforcing efficiency of single-walled carbon nanotubes in oriented poly(vinyl alcohol) tapes. Nanotechnology. 2007(45):455709.

31. Minus ML, Chae HG, Kumar S. Single wall carbon nanotube templated oriented crystallization of poly(vinyl alcohol). Polymer. 2006;47(11):3705-10.

32. Vollrath F, Knight DP. Liquid crystalline spinning of spider silk. Nature. 2001;410(6828):541-8.

33. Han Gi Chae SK. Rigid-rod polymeric fibers. Journal of Applied Polymer Science. 2006;100(1):791-802.

Table of figures